

# Second harmonic generation in a low-loss orientation-patterned GaAs waveguide

K. A. Fedorova,<sup>1,\*</sup> A. D. McRobbie,<sup>2</sup> G. S. Sokolovskii,<sup>1,3</sup> P. G. Schunemann,<sup>4</sup>  
and E. U. Rafailov<sup>1</sup>

<sup>1</sup>Photonics & Nanoscience Group, School of Engineering, Physics and Mathematics, University of Dundee, DDI 4HN, UK

<sup>2</sup>Currently with Selex Galileo Inc., Crewe Toll Phase 1, Edinburgh, EH5 2XS, UK

<sup>3</sup>Ioffe Physico-Technical Institute, 26 Polytechnicheskaya Str., St. Petersburg, 194021, Russia

<sup>4</sup>BAE Systems, P.O. Box 868, MER15-1813, Nashua, NH 03061-0868, USA

\*K.A.Fedorova@dundee.ac.uk

**Abstract:** The technology of low-loss orientation-patterned gallium arsenide (OP-GaAs) waveguided crystals was developed and realized by reduction of diffraction scattering on the waveguide pattern. The propagation losses in the OP-GaAs waveguide were estimated to be as low as 2.1 dB/cm, thus demonstrating the efficient second harmonic generation at 1621 nm under an external pumping.

©2013 Optical Society of America

**OCIS codes:** (190.0190) Nonlinear optics; (190.2620) Harmonic generation and mixing; (230.7370) Waveguides.

---

## References and links

1. C. Wang and P. Sahay, "Breath analysis using laser spectroscopic techniques: Breath biomarkers, spectral fingerprints, and detection limits," *Sensors (Basel)* **9**(10), 8230–8262 (2009).
2. M. J. Thorpe, D. Balslev-Clausen, M. S. Kirchner, and J. Ye, "Cavity-enhanced optical frequency comb spectroscopy: application to human breath analysis," *Opt. Express* **16**(4), 2387–2397 (2008).
3. M. A. Mackanos, D. M. Simanovskii, K. E. Schriver, M. Hutson, C. H. Contag, J. A. Kozub, and E. Duco Jansen, "Pulse-duration-dependent mid-infrared laser ablation for biological applications," *IEEE J. Sel. Top. Quantum Electron.* **18**(4), 1514–1522 (2012).
4. C. Eliasson, N. A. Macleod, and P. Matousek, "Noninvasive detection of concealed liquid explosives using Raman spectroscopy," *Anal. Chem.* **79**(21), 8185–8189 (2007).
5. A. Hugi, R. Maulini, and J. Faist, "External cavity quantum cascade laser," *Semicond. Sci. Technol.* **25**(8), 083001 (2010).
6. T. Kruczek, K. A. Fedorova, G. S. Sokolovskii, R. Teissier, A. N. Baranov, and E. U. Rafailov, "InAs/AlSb widely tunable external cavity quantum cascade laser around 3.2  $\mu\text{m}$ ," *Appl. Phys. Lett.* **102**(1), 011124 (2013).
7. M. M. Fejer, G. A. Magel, D. H. Jundt, and R. L. Byer, "Quasi-phase-matched second harmonic generation: tuning and tolerances," *IEEE J. Quantum Electron.* **28**(11), 2631–2654 (1992).
8. D. V. Petrov, "Nonlinear phase shift by cascaded quasi-phase-matched second harmonic generation," *Opt. Commun.* **131**(1-3), 102–106 (1996).
9. I. Shoji, T. Kondo, A. Kitamoto, M. Shirane, and R. Ito, "Absolute scale of second-order nonlinear-optical coefficients," *J. Opt. Soc. Am. B* **14**(9), 2268–2294 (1997).
10. F. A. Katsriku, B. M. A. Rahman, and K. T. V. Grattan, "Numerical modeling of second harmonic generation in optical waveguides using the finite element method," *IEEE J. Quantum Electron.* **36**, 282–289 (2000).
11. L. Gordon, G. L. Woods, R. C. Eckardt, R. R. Route, R. S. Feigelson, M. M. Fejer, and R. L. Byer, "Diffusion-bonded stacked GaAs for quasiphasematched second-harmonic generation of a carbon dioxide laser," *Electron. Lett.* **29**(22), 1942–1944 (1993).
12. S. J. B. Yoo, R. Bhat, C. Caneau, and M. A. Koza, "Quasi-phase-matched second-harmonic generation in AlGaAs waveguides with periodic domain inversion achieved by wafer-bonding," *Appl. Phys. Lett.* **66**(25), 3410–3412 (1995).
13. S. J. B. Yoo, C. Caneau, R. Bhat, M. A. Koza, A. Rajhel, and N. Antoniadis, "Wavelength conversion by difference frequency generation in AlGaAs waveguides with periodic domain inversion achieved by wafer bonding," *Appl. Phys. Lett.* **68**(19), 2609–2611 (1996).
14. E. U. Rafailov, P. Loza-Alvarez, C. T. A. Brown, W. Sibbett, R. M. De La Rue, P. Millar, D. A. Yanson, J. S. Roberts, and P. A. Houston, "Second-harmonic generation from a first-order quasi-phase-matched GaAs/AlGaAs waveguide crystal," *Opt. Lett.* **26**(24), 1984–1986 (2001).
15. D. Artigas, E. U. Rafailov, P. Loza-Alvarez, and W. Sibbett, "Periodically switched nonlinear structured for frequency conversion: theory and experimental demonstration," *IEEE J. Quantum Electron.* **40**(8), 1122–1130 (2004).

16. S. Koh, T. Kondo, T. Ishiwada, C. Iwamoto, H. Ichinose, H. Yaguichi, T. Usami, Y. Shiraki, and R. Ito, "Sublattice Reversal in GaAs/Si/GaAs (100) Heterostructures by Molecular Beam Epitaxy," *Jpn. J. Appl. Phys.* **37**(Part 2, No. 12B), L1493–L1496 (1998).
17. C. B. Ebert, L. A. Eyres, M. M. Fejer, and J. S. Harris, Jr., "MBE growth of antiphase GaAs films using GaAs/Ge/GaAs heteroepitaxy," *J. Cryst. Growth* **201-202**, 187–193 (1999).
18. T. Kondo, S. Koh, and R. Ito, "Sublattice reversal epitaxy: a novel technique for fabricating domain-inverted compound semiconductor structures," *Sci. Technol. Mater.* **1**(3), 173–179 (2000).
19. P. Schunemann, "CdSiP<sub>2</sub> and OPGaAs: New nonlinear crystals for the mid-infrared," in *Advances in Optical Materials*, OSA Technical Digest (Optical Society of America, 2011), paper AIFA1, (2011).
20. M. B. Oron, S. Pearl, P. Blau, and S. Shusterman, "Efficient second-harmonic generation and modal dispersion effects in orientation-patterned GaAs waveguides," *Opt. Lett.* **35**(16), 2678–2680 (2010).
21. S. Strite, D. Biswas, N. S. Kumar, M. Fradkin, and H. Morkoc, "Antiphase domain free growth of GaAs on Ge in GaAs/Ge/GaAs heterostructures," *Appl. Phys. Lett.* **56**(3), 244–246 (1990).
22. M. B. Oron, S. Shusterman, and P. Blau, "Periodically oriented GaAs templates and waveguide structures for frequency conversion," *Proc. SPIE* **6875**, 68750F, 68750F-12 (2008).
23. J. Ota, W. Narita, I. Ohta, T. Matsushita, and T. Kondo, "Fabrication of periodically-inverted AlGaAs waveguides for quasi-phase-matched wavelength conversion at 1.55  $\mu\text{m}$ ," *Jpn. J. Appl. Phys.* **48**(4), 04C110 (2009).
24. D. A. Yanson, E. U. Rafailov, G. S. Sokolovskii, V. I. Kuchinskii, A. C. Bryce, J. H. Marsh, and W. Sibbett, "Self-focussed distributed Bragg reflector laser diodes," *J. Appl. Phys.* **95**(3), 1502–1509 (2004).
25. V. V. Dudelev, G. S. Sokolovskii, S. N. Losev, A. G. Deryagin, V. I. Kuchinskii, S. A. Nikishin, M. Holtz, E. U. Rafailov, and W. Sibbett, "Phase effects in broad-area heterolasers with curved grooves of distributed feedback grating," *Tech. Phys. Lett.* **33**, 292–293 (2007).
26. G. P. Agrawal, *Nonlinear Fiber Optics* (Academic, 1989).

## 1. Introduction

The development of compact, low-cost broadly-tunable coherent sources in the mid-infrared spectral range (3 - 16  $\mu\text{m}$  and beyond) can provide indispensable tools for a variety of scientific, technological and industrial applications, including biomedicine, spectroscopy, trace gas sensing [1–3], and potentially for the detection of concealed explosive materials [4]. The devices presently used for this spectral range are typically based on narrow band-gap semiconductors and quantum cascade lasers [5,6], but these are restricted to a limited tunability range. Considerable progress over the last few years in material science, crystal growth and semiconductor material processing, combined with recent advances in some of the more traditional technologies - in particular nonlinear frequency conversion and parametric sources - have led to the realization of a new generation of high-performance laser sources.

Recent progress in the development of periodic-poling techniques for patterning the domain structure of ferroelectric materials (LiNbO<sub>3</sub>, LiTaO<sub>3</sub>, KTiOPO<sub>4</sub>) has led to the implementation of different quasi-phase-matched (QPM) structures for efficient nonlinear optical interactions [7]. Meanwhile, semiconductor materials such as GaAs and AlAs and their alloys are especially promising for infra-red (IR) applications, because of their high transparency in the IR region (from 1  $\mu\text{m}$  to 16  $\mu\text{m}$  [8]), large nonlinear coefficients and high thresholds for optical damage. For example, GaAs exhibits a very broad optical transparency, extending from 870 nm through to 16  $\mu\text{m}$  and has nonlinearity as large as  $d_{14} = 119 \text{ pm/V}$  at 1.53  $\mu\text{m}$  wavelength [9]. However, GaAs-based materials have very high absorption losses particularly at shorter wavelengths [10]. Therefore, the periodically poled design in GaAs semiconductor structure is better suited to, and can be successfully realized for frequency conversion (second harmonic generation or optical parametric oscillator) into the near- and mid-infrared spectral region up to 16  $\mu\text{m}$ .

The optically isotropic, non-ferroelectric nature of GaAs makes it unsuitable for common phase-matching methods based on birefringence or periodic poling and so alternative methods to utilize it as a medium for nonlinear optical frequency conversion have been implemented, including diffusion-bonded GaAs stack of plates [11], direct wafer bonding for periodically domain-inverted AlGaAs [12,13] and periodically-switched-nonlinearity method in a semiconductor structure [14,15] using either an ion-implantation technique or an etch and re-growth process.

To address this issue, a novel technology has been developed for QPM of semiconductors - so-called orientation-patterning (OP) [16–18] - which allows the fabrication of high quality domain inverted semiconductor structures (for example, periodically-poled GaAs based crystals [19,20]) which demonstrate significantly better conversion efficiencies. The idea of this technology is to deposit a thin non-polar buffer layer (such as germanium, which has a very similar lattice constant to GaAs with  $\sim 0.1\%$  mismatch [21]) to reverse sublattice occupation, followed by subsequent overgrowth of GaAs layer in antiphase to the substrate. Without this buffer layer, deposited GaAs layers nucleate in the same orientation as the preceding layer. Selective removal of inverted GaAs material and buffer layers followed by MBE regrowth allows the creation of positive and negative material in a side-by-side all-epitaxially grown structure. Regions of domain-inverted material exhibit sign reversal of all their non-vanishing nonlinear coefficients resulting in a nonlinear coefficient variation identical to the case of periodically poled ferroelectric crystals, to provide forward conversion at each coherence length. No wafer bonding is utilized in this technology, making it robust and very attractive in comparison with even the most sophisticated and mature of the earlier developed techniques [20], which involve several process steps to minimize roughness and defect density at the grown layers interfaces for deposition of high quality waveguide layer stacks on OP-GaAs templates [22].

Furthermore, ridge waveguide configuration can be employed to ensure good optical confinement and efficient nonlinear conversion and thus permit the exploitation of low power pump sources (potentially diode lasers). Moreover, the fabrication of OP-GaAs waveguided devices requires shorter growth time and is cheaper in comparison with bulk devices. Therefore, the waveguide design of orientation-patterned semiconductor structure [20,23] is better suited to, and can be successfully realized for the development of new all-semiconductor frequency conversion and parametric sources with previously unattainable performance capabilities.

Here we present our results on the investigation of frequency conversion in OP-GaAs waveguides. The technology of low-loss “periodically poled” waveguided crystals with a 6  $\mu\text{m}$  GaAs layer was developed and realized. These periodically-domain inverted GaAs waveguided devices differ from the previously reported in the material structure [16–18,23] or in the growth and fabrication techniques [20]. The performance of the optimized low-loss OP-GaAs waveguides was investigated and second harmonic generation (SHG) at 1621 nm in such device was demonstrated. A loss value as low as 2.1 dB/cm was measured, which is comparable to the lowest losses reported to date for an OP-GaAs waveguide [20]. For this proof-of-principle work, an optical parametric oscillator (OPO) system was developed as a pump source. It was based on a periodically poled 5 mol% MgO-doped Congruent Lithium Niobate (PPLN) crystal, generating light in the wavelength range between 1430 nm and 4157 nm.

## 2. OP-GaAs sample fabrication

### 2.1 Waveguide design

When designing the OP-GaAs structure and waveguide, we first aimed to reduce the propagation losses of the system to the level of a few dB/cm, which is necessary for any practical application. These losses are typically associated mainly with (i) scattering due to the low quality of interfaces of the orientation-patterning and (ii) diffractive out-coupling of the waveguide modes due to corrugation of the waveguide, associated with formation of the contrary-oriented GaAs patterns. Manufacture of the orientation-patterned structure involved considerable efforts to improve the interfaces quality and totally eliminate unwanted corrugations of the waveguide. However, the latter appeared to be technically impossible due to involvement of the extra layer (Ge) underlying the inverted patterns (see Section 2.2). Therefore, thoughtful engineering of the OP-GaAs structure was crucial for reduction of the diffraction losses to an acceptable level.

The effect of the waveguide corrugation on the diffraction out-coupling was found to be a function of not only the corrugation depth, but also the composition of the waveguide barriers and thickness of the waveguide. Mode confinement (the reason for dependence of the diffraction losses on the waveguide parameters, as discussed) was analyzed not only for the fundamental TE mode [20] but also for its higher-order counterparts. This research revealed the strong dependence of waveguide losses on the optical alignment, which was later confirmed experimentally.

Our analysis of the light propagation through the OP-GaAs structure was based on the scalar linear theory [24,25] and involved only material parameters alongside the wavelength  $\lambda$ , corrugation depth  $\Delta d$  and the effective refractive index of the waveguide  $N_{\text{eff}}$ . The last parameter was calculated numerically in the thin-film approximation, which was well applicable with the planned ridge width of  $15\mu\text{m}$ . With this approximation, waveguide thickness  $d$  and the waveguide barrier  $\text{Al}_x\text{Ga}_{1-x}\text{As}$  composition  $x$  were directly included into the calculation of the diffraction losses through the effective refractive index  $N_{\text{eff}}$ .

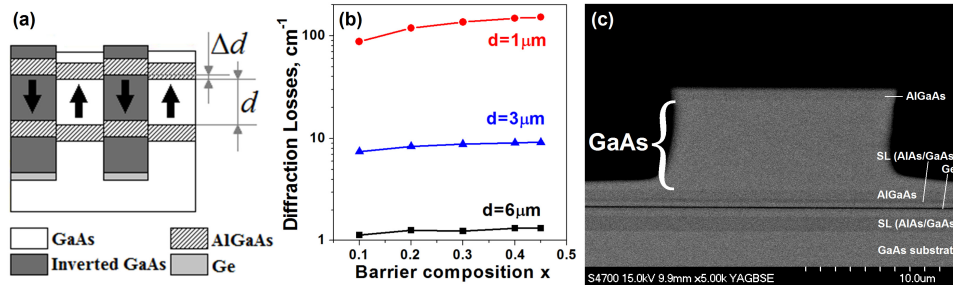


Fig. 1. (a) Profile of the OP-GaAs structure. (b) Calculated diffraction losses of the fundamental TE mode vs composition of the  $1\mu\text{m}$ ,  $3\mu\text{m}$  and  $6\mu\text{m}$ -thick  $\text{Al}_x\text{Ga}_{1-x}\text{As}/\text{GaAs}$  waveguide with corrugation depth  $\Delta d = 150\text{nm}$ . (c) SEM image of the fabricated OP-GaAs waveguide.

Figures 1(a) and 1(b) show the modeled profile of the OP-GaAs waveguide and calculated dependence of the diffraction losses on the waveguide composition  $x$  for the fundamental TE mode. From these figures, one can note the contra-intuitive increase of the waveguide losses with increase of the ‘heights’ of the waveguide barrier. This behavior of the diffraction losses can be understood if the mode confinement is taken into account. Indeed, distribution of the weaker confined optical field (low  $x$ ) is less affected by the corrugation of the waveguide than that of its better confined counterpart (high  $x$ ).

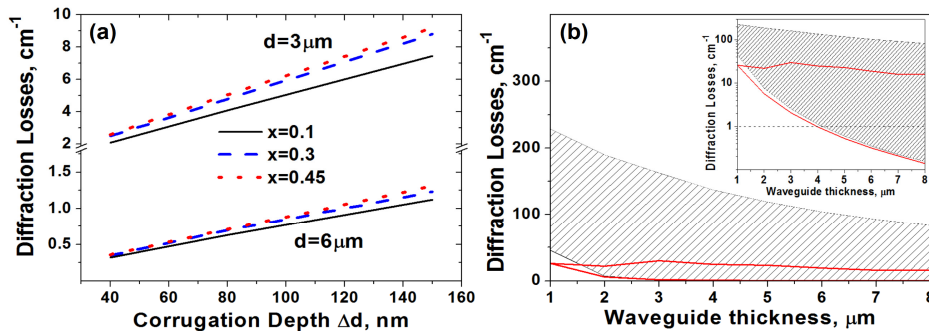


Fig. 2. (a) Diffraction losses of the fundamental TE mode vs corrugation depth for  $d = 3\mu\text{m}$  and  $d = 6\mu\text{m}$  for  $\text{Al}_x\text{Ga}_{1-x}\text{As}$  barrier compositions  $x = 0.1$ ,  $x = 0.3$  and  $x = 0.45$ . (b) Diffraction losses of the different-order modes vs waveguide thickness for  $\Delta d = 40\text{nm}$  for  $x = 0.45$  (black) and  $x = 0.1$  (red). The range of possible diffraction losses increasing from the fundamental TE to the higher-order modes is shown in (b) with hatch. Inset: log-scale zoom in.

In Fig. 2 the dependence of diffraction losses on the waveguide thickness and the depth of corrugation are shown. It is important to note that the options to achieve practical value of losses with deep corrugation  $\Delta d$  (thick Ge layer) are very limited even for very broad waveguides and vice-versa narrow waveguides are prone of high diffraction losses. This is in-line with our earlier experiments as well as [23] demonstrating 9dB/cm losses for 3 $\mu$ m-thick waveguide. On the other hand, taking into account higher-order modes shows the importance of the optical alignment for reduction of diffraction losses. With broad waveguides, a number of higher-order modes can be involved in light propagation, leading to completely different diffraction losses with the same light coupling efficiency. The range of possible diffraction losses increasing from zero- to the high-order modes is shown with hatch in Fig. 2(b). One can see that reduction of the Al<sub>x</sub>Ga<sub>1-x</sub>As barrier heights can dramatically reduce the range of the alignment-defined waveguide losses, which we found to be very important in our experiments.

## 2.2 Sample fabrication

According to our calculations (see Section 2.1), the epitaxial layer structure of OP-GaAs devices was optimized in order to reduce the propagation losses. The fabrication of the OP-GaAs samples involved a few steps. First, growth was initiated on a (100) GaAs substrate misoriented 4° towards (111) with an AlAs/GaAs superlattice buffer growth (~1  $\mu$ m). Then the 1000Å layer of GaAs and 200Å of Al<sub>0.75</sub>Ga<sub>0.25</sub>As were grown, and after that the growth was completed by a 100Å layer of GaAs. Then a buffer layer of Ge (40Å) was grown on top of the GaAs, followed by growth of a 1200Å GaAs layer, whose crystallographic orientation is rotated 90° around the  $\bar{1}00$  direction with respect to the substrate equivalent to an inversion in the  $\bar{4}3m$  zinc-blende structure. Then 200Å of Al<sub>0.75</sub>Ga<sub>0.25</sub>As and 200Å of GaAs were grown to protect the GaAs layer from contaminants such as photoresist used for patterning of QPM gratings.

Exposure and development of a photoresist etch mask (with appropriate designed periods) followed by chemical or ion beam etching down to the GaAs layer that lay below Ge layer which produced an orientation grating pattern across the wafer surface. The patterned orientation template produced by such a process after appropriate cleaning was then placed back into the MBE system for re-growth of a thick layer of GaAs (0.25  $\mu$ m) to produce an OP-GaAs template, which was covered by AlAs/GaAs superlattice buffer layer (0.25 $\mu$ m) and then Al<sub>0.3</sub>Ga<sub>0.7</sub>As (0.2 $\mu$ m) and Al<sub>0.1</sub>Ga<sub>0.9</sub>As (0.5 $\mu$ m) deposition to form the lower waveguiding layer. The next phase in the manufacture was re-growth to form the active region of GaAs (6 $\mu$ m) and subsequent Al<sub>0.1</sub>Ga<sub>0.9</sub>As (0.5 $\mu$ m) and Al<sub>0.3</sub>Ga<sub>0.7</sub>As (0.2 $\mu$ m) deposition to form the upper waveguiding layer and complete the optical waveguide in the vertical direction. At the final stage of the sample preparation, the 15 $\mu$ m-wide waveguides were defined in the material in a direction perpendicular to the grating using Chemically Assisted Ion Beam Etching. Very high beam voltages of around 1800 V in conjunction with low beam currents of around 20 mA were utilized to produce the type of the high quality, high aspect ratio trenches required for such devices. The material was etched down to a depth of ~6  $\mu$ m to define the mesa waveguides. The SEM image of a fabricated OP-GaAs waveguide is shown in Fig. 1(c).

## 3. Experimental results

In order to investigate the frequency conversion properties of the orientation-patterned GaAs waveguides, a continuously tunable laser source was required. For this purpose an OPO system based on a PPLN crystal and pumped by a Q-switched Nd:YAG laser was built. The Nd:YAG laser had a wavelength of 1064 nm, a maximum pulse energy of 30  $\mu$ J, a pulse duration of 15 ns and 10 kHz repetition rate. The combined signal and idler spectra continuously covered the spectral range between 1430 nm and 4157 nm. The maximum idler average output power of 10.5 mW and idler slope efficiency of 6.13% at 3242 nm were achieved for 250 mW of pump power at 1064 nm. The total generated power of the signal and

idler waves was 12.38 mW. This corresponded to a pump power of 250 mW and a total down-conversion slope efficiency of 7.2%. This OPO system was used as the pump source for SHG in OP-GaAs waveguide. The output of the OPO system was coupled using a 40x aspheric lens (NA of 0.55) in an OP-GaAs waveguide with temperature controlled by a thermo-electric cooler. The SHG output was collected using a similar aspheric lens.

An OP-GaAs waveguide with a length of  $\sim 4$  mm and a width of  $15 \mu\text{m}$  was selected to examine the possibility of obtaining second harmonic generation. According to our calculation, a wavelength of 3242 nm was chosen as a suitable pump for the OP-GaAs waveguide sample with a coherence length of  $14.5 \mu\text{m}$  (grating period of  $29 \mu\text{m}$ ). The spectra of the fundamental (3242 nm) and SHG (1621 nm) wavelengths were measured with a monochromator and PbSe Photoconductive detector, as shown in the inset to Fig. 3(a). The optical spectrum of the fundamental and second harmonic waves exhibited a bandwidth of around 5.1 nm and 1.2 nm, respectively. For measurements of the frequency doubled light, a high speed InGaAs detector assisted via a lock-in amplifier was used to detect the SHG signal. The SHG intensity is plotted in Fig. 3(a) as a function of the pump power of the fundamental wavelength launched into the OP-GaAs waveguide. The data shows the expected quadratic response for the SHG process, as can be seen from the linear fit which has a slope of  $\sim 1.91$  (Fig. 3(a)). The SHG signal vanished when the polarization of the fundamental wavelength was rotated by  $90^\circ$ .

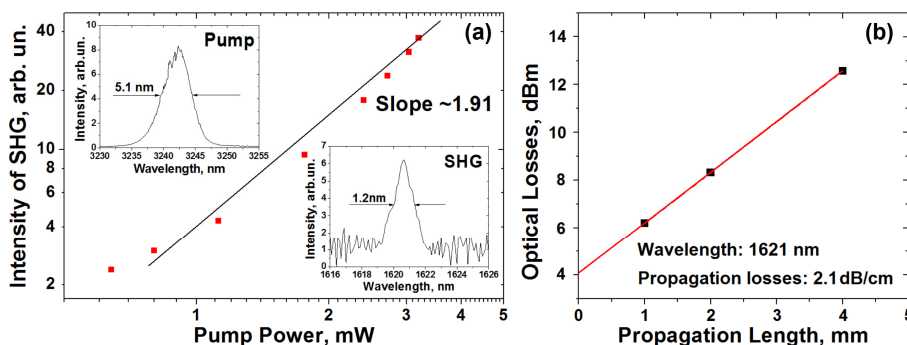


Fig. 3. (a) Second harmonic intensity as a function of fundamental input power. Inset: Spectra of the pump and SHG waves. (b) Total insertion loss measured using the cutback method.

OP-GaAs waveguide loss measurements were made using the cutback method [26]. The OP-GaAs waveguides used in this work were identical and had a width of  $15 \mu\text{m}$  and 3 different lengths: 4 mm, 2 mm and 1 mm. The 1621 nm wavelength from the OPO system was chosen as a pump for the OP-GaAs waveguide loss measurements. From Fig. 3(b), insertion losses were estimated to be  $\sim 4$  dB and the propagation losses - around 2.1 dB/cm. The latter is comparable to the lowest losses reported to date for OP-GaAs waveguides [20].

#### 4. Conclusion

The investigations undertaken in our work sought to evaluate the suitability of newly developed orientation-patterning technique to fabricate low-loss “periodically poled” GaAs waveguided devices for nonlinear frequency conversion, as the laser sources based on the orientation-patterned semiconductor crystals can be suitable for studies in gas sensing, atmospheric transmission, telecommunications and medical applications.

For this purpose, the technology of low-loss orientation-patterned GaAs waveguided crystals was developed and realized. In order to optimize the waveguide design and minimize the propagation losses, the calculation of diffraction light out-coupling from such waveguides was undertaken which enabled demonstration of losses as low as 2.1 dB/cm. Using the extremely versatile home-made OPO system as a pump source, frequency doubled light at 1621 nm in a low-loss orientation-patterned GaAs waveguide was demonstrated. In our future work, we will use antireflection coatings on the crystal facets which, along with optimization

of the focusing optics, will minimize coupling losses and assist in further improvement of the system.

Here we have shared extremely promising results for fabrication of high-performance frequency conversion devices by orientation-patterned GaAs waveguides. Their further optimization can lead to realization of significantly more power efficient laser devices and allow us to extend the generated wavelength up to 16  $\mu\text{m}$  with all-semiconductor optical parametric oscillation technology.

### **Acknowledgments**

This work was supported by the Engineering and Physical Sciences Research Council (EPSRC).